

Thermo- and fluid dynamic model of a multiphase screw pump, operating at very high gas volume fractions

Dipl.-Ing. (FH) Klaus Rübiger
Prof. Dr. T.M.A. Maksoud
Prof. Dr. John Ward

University of Glamorgan
School of Technology
Wales, UK

Prof. Dr. G. Hausmann

Georg-Simon-Ohm Fachhochschule Nürnberg
Fachbereich Maschinenbau und
Versorgungstechnik

Abstract

To describe the performance as well as the thermodynamic behaviour of a multiphase screw pump, also operating at very high gas volume fractions up to 100 %, a new thermo- and fluid dynamic model was developed. The model, which will be presented in this paper, takes the time-dependent gas-liquid heat transfer, the compressibility and acceleration effects of the multiphase gap flow as well as the possibility of critical flow conditions into account. For the simulation of the mutual phase heat transfer, the solution of the gap flow conservation equations and the optimisation of the gap inflow velocity, different numerical techniques were used. The model as such gives important information of the pressure and the temperature distribution, the multiphase leakage flows through the chamber connecting gaps as well as the effective flow rate or the volumetric efficiency of the pump near the conveyance break-off at very high gas volume fractions.

Key words : screw pump - multiphase - gas volume fraction

1. Introduction

A screw pump is a particular type of rotary displacement pumps, in which a number of screws rotate inside a cylindrical housing. The geometry and rotation of the screws generate a series of closed chambers, which transport the fluid from the low pressure inlet to the high pressure outlet. The pressure distribution through the pump and hence the flow characteristics and system performance is heavily influenced by the leakage flow from the discharge side to the suction side. This leakage flow occurs through three different gaps inside the screw pump, namely the perimeter gap between the screws and the housing, and the radial and flank gap between the mating surfaces of the screws, see Figure 1.1.

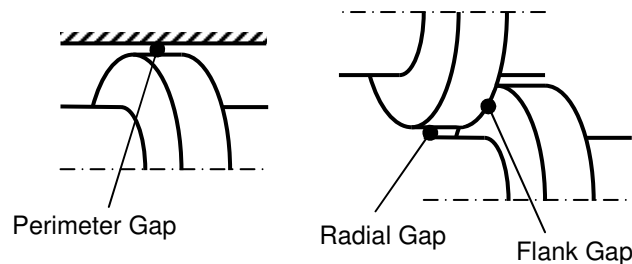


Figure 1.1 : Three different kind of gaps inside the screw pump

Previous investigations of multiphase screw pumps have largely been concerned with the general pumping behaviour of these systems [1]. Moreover these studies have been restricted to relatively medium sized pumps, in which the maximum power consumption and gas concentrations are relatively modest. In these situations the heat capacity and density of the gas-liquid mixture is dominated by the liquid phase so that the pumping process is essentially isothermal and thermodynamic effects can be neglected [2] and [3]. However, this assumption cannot be justified for larger, more powerful screw pumps, which are capable of conveying two-phase fluids with very high concentrations of the gaseous phase up to 100 %. There are existing two new models [4] and [5], which include the thermodynamic effects by establishing mass and energy balance equations for each chamber. But no multiphase screw pump model can be found in literature, which deals with the compressibility or the critical flow condition of the two-phase leakage flow through the gaps. Due to the above-mentioned lack of the correct modelling of compressibility effects, acceleration pressure drops and critical flow conditions, it is necessary to create a model for compressible gap flows inside of multiphase screw pumps, using analytical and numerical methods, to predict the leakage flow and the thermal behaviour more accurately.

2. Chamber model of the screw pump

The thermodynamic screw pump model can be treated as a collection of several chambers, which are connected by three different kinds of gaps. Due to the nature of a positive displacement pump - except for the leakage amount, the theoretical volume flow is constant at all times - only the leakage flow has to be investigated, to determine the real volume flow or the volumetric efficiency factor. The driving forces for leakage are the local pressure difference between two corresponding chambers and the rotating screws. Because of the rotation of the screws, the chambers are transported from the suction to the discharge side of the pump. In a real screw pump, the leakage flow increases the pressure in all the chambers incrementally from the inlet to the outlet. In the case of 100 % liquid phase, the pressure distribution is linear, because the fluid is incompressible and a certain amount of leakage at the pump outlet must have the same amount of leakage, which flows out at the pump inlet. But if the gas volume fraction increases and the chambers are allowed to have different gas volume fractions, the pressure profile becomes non-linear. The shape depends mainly on the gas volume fraction and the rotational speed of the screws. To determine the correct pressure and temperature profiles etc. along the screw axis, the chamber inflow and outflow process have to be investigated for all chambers, beginning at the pump discharge side. The correct chamber connection between the suction (S) and the discharge (D) of a double-flight twin screw pump through the perimeter gap (PG) and the radial gap (RG) is shown in Figure 2.1. As a consequence of the minor contribution of the flank gap to the whole leakage mass flow, the flank gap was not considered in the current model.

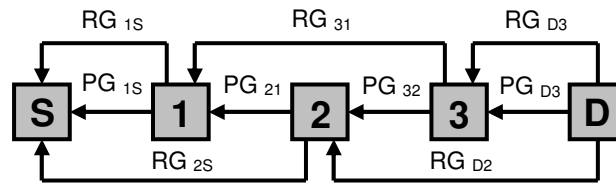


Figure 2.1 : Chamber connection scheme of a double-flight twin screw pump (here with 3 chambers)

The investigation time, which is divided into small time steps, is equal to the life time of the chambers. After this period, all chambers move one chamber position in the outlet direction. This means, that the former last chamber No. 3 have opened to the high pressure side and there is now a complete new chamber No. 1. The iteration of chamber changes, which includes all sub-iterations, has to be carried out so long, until all thermodynamic chamber variables reach a steady state. In the case of an odd number of chambers, the real pumping behaviour has to be determined by a weighting procedure between the next even upper and lower chamber number, depending on their temporal occurrence. The calculation of the thermodynamic conditions of a single chamber can be splitted into the following working stages, see also Figure 2.2:

- a) **Gas inflow** (constant specific total enthalpy)
- b) **Liquid inflow** (constant specific total enthalpy)
- c) **Gas compression by liquid inflow** (gas temperature increasing)
- d) **Liquid outflow** (variable specific total enthalpy)
- e) **Gas expansion by liquid outflow** (gas temperature decreasing)
- f) **Gas outflow** (variable specific total enthalpy)
- g) **Gas-liquid heat transfer** (through the interfacial area)

The chamber conditions of both phases and also the volume fractions, after the inflow (intermediate stage) and after the outflow process (final stage) are calculated iteratively. The division of the total inflow and outflow process into small time steps assures a nearly continuous flow through all chambers.

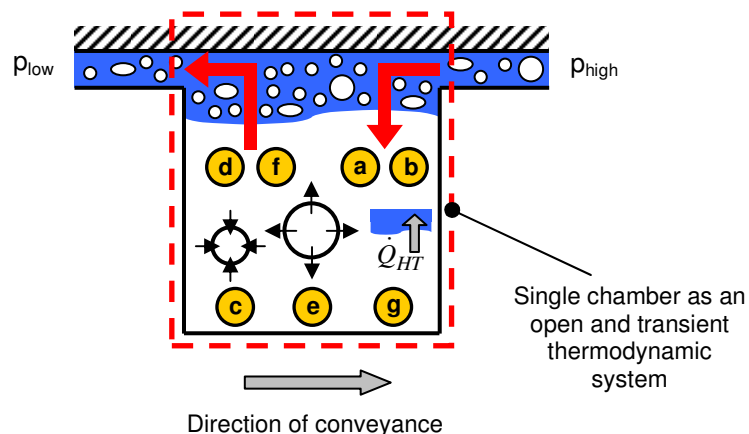


Figure 2.2 : Open and transient thermodynamic system

3. Fundamental thermodynamic equations for open systems

Each chamber of the screw pump was modelled as a thermodynamic open system [6] and [7], whereas the inflow and the escape of single or two-phase fluid from one chamber to the other are considered as transient processes. To describe the thermodynamic changes of the chamber condition, mass and energy conservation equations have to be applied, which were derived and introduced in this and the next sections.

$$Q_{12} + W_{12} = E_{total,2} - E_{total,1} \quad \text{First law of thermodyn.} \quad (3.1)$$

$$E_{total} = U + E_{kin} + E_{pot} \quad \text{Total energy} \quad (3.2)$$

$$U = U_{cha} + \Delta m_{in/out} \cdot u_{in/out} \quad \text{Internal energy} \quad (3.3)$$

$$E_{kin} = E_{kin,cha} + \Delta m_{in/out} \cdot \frac{w_{in/out}^2}{2} \quad \text{Kinetic energy} \quad (3.4)$$

$$E_{pot} = E_{pot,cha} + \Delta m_{in/out} \cdot g \cdot z_{in/out} \quad \text{Potential energy} \quad (3.5)$$

$$W_{12} = W_{tech,12} + p_{in} \cdot v_{in} \cdot \Delta m_{in} - p_{out} \cdot v_{out} \cdot \Delta m_{out} \quad \text{System work} \quad (3.6)$$

The energy conservation equation follows from the first law of thermodynamics for transient processes in open systems for a negligible kinetic and potential energy of the chamber itself to

$$\begin{aligned} m_{cha,2} \cdot u_{cha,2} - m_{cha,1} \cdot u_{cha,1} &= Q_{12} + W_{tech,12} \\ + \left(h_{in} + \frac{w_{in}^2}{2} + g \cdot z_{in} \right) \cdot \Delta m_{in} &- \left(h_{out} + \frac{w_{out}^2}{2} + g \cdot z_{out} \right) \cdot \Delta m_{out} \end{aligned} \quad (3.7)$$

The heat transfer and the technical work concerning the chambers were not implemented in the current adiabatic model stage for the simulation of non-decreasing chamber volumes. Nevertheless, both contributions were introduced here for completeness and to enable a future implementation. The time span for determining the different mass flows in and out of the chamber has to be chosen sufficiently small, in the following example to 0.2 ms, so that the final pressure and temperature distribution become almost independent of any further time reduction of each sub-iteration and has to be adapted in certain circumstances, depending on the operating point of the screw pump.

4. Chamber inflow process

The chamber inflow process consists of the inflow of the gaseous phase, then the inflow of the liquid phase - both at constant specific total enthalpy - and finally the gas compression by the increased liquid volume. At any stage, both fluids are sharing the same pressure value and during the inflow, the multiphase fluid is not able to flow out of the chamber. Furthermore, the process can be assumed as adiabatic, with no applied work energy from outside and a negligible difference in potential energy. The chamber inflow is mathematically described below in a sequential manner.

• **Formulas for the chamber inflow**

$$m_{cha,2} \cdot u_{cha,2} - m_{cha,1} \cdot u_{cha,1} = \left(h_{in} + \frac{w_{in}^2}{2} \right) \cdot \Delta m_{in} \quad (4.1)$$

$$m_{cha,2} = m_{cha,1} + \Delta m_{in} \quad \text{conservation of mass} \quad (4.2)$$

$$\left(h_{in} + \frac{w_{in}^2}{2} \right) = e = \text{const.} \quad \text{constant total spec. enthalpy} \quad (4.3)$$

$$\frac{m_{cha,2}}{m_{cha,1}} = \frac{e - u_{cha,1}}{e - u_{cha,2}} \quad \text{chamber inflow equation} \quad (4.4)$$

• **Gas inflow**

$$\frac{m_{cha,G,2}}{m_{cha,G,1}} = \frac{c_{p,G} \cdot T_{in} + \frac{w_{in}^2}{2} - c_{v,G} \cdot T_{cha,G,1}}{c_{p,G} \cdot T_{in} + \frac{w_{in}^2}{2} - c_{v,G} \cdot T_{cha,G,2}} \quad \text{resulting in } T_{cha,G,2} \quad (4.5)$$

$$\frac{m_{cha,G,2}}{m_{cha,G,1}} = \frac{p_{cha,2} \cdot T_{cha,G,1}}{p_{cha,1} \cdot T_{cha,G,2}} \quad \text{resulting in } p_{cha,2} \quad (4.6)$$

• **Liquid inflow**

$$\frac{m_{cha,L,2}}{m_{cha,L,1}} = \frac{T_{in} + \frac{w_{in}^2}{2 \cdot c_L} - T_{cha,L,1}}{T_{in} + \frac{w_{in}^2}{2 \cdot c_L} - T_{cha,L,2}} \quad \text{resulting in } T_{cha,L,2} \quad (4.7)$$

• **Gas compression by liquid inflow**

$$V_{cha,G,1} = \alpha_{cha,2} \cdot V_{cha} + \frac{\Delta m_{in,L}}{\rho_L} \quad \text{gas volume - before} \quad (4.8)$$

$$V_{cha,G,2} = \alpha_{cha,2} \cdot V_{cha} \quad \text{gas volume - after} \quad (4.9)$$

$$p_2 = p_1 \cdot \left(\frac{V_{cha,G,1}}{V_{cha,G,2}} \right)^\kappa \quad \text{isentropic change of pressure} \quad (4.10)$$

$$T_{G,2} = T_{G,1} \cdot \left(\frac{V_{cha,G,1}}{V_{cha,G,2}} \right)^{(\kappa-1)} \quad \text{isentropic change of temp.} \quad (4.11)$$

5. Chamber outflow process

The chamber outflow process consists of the outflow of the liquid phase at variable specific total enthalpy, then the gas expansion by the decreasing liquid volume and finally the gas outflow also at variable specific total enthalpy. As in the case for inflow process, both fluids are sharing the same pressure value and during the outflow, multiphase fluid is not able to flow into the chamber. Furthermore, the process can also be assumed as adiabatic, with no applied work energy from outside and a negligible difference in potential energy. The chamber outflow is mathematically described below also in a sequential manner.

• Formulas for the chamber outflow

$$m_{cha,1} \cdot u_{cha,1} - m_{cha,2} \cdot u_{cha,2} = \left(h_{out} + \frac{w_{out}^2}{2} \right) \cdot \Delta m_{out} \quad (5.1)$$

$$m_{cha,1} - m_{cha,2} = \Delta m_{out} \quad \text{conservation of mass} \quad (5.2)$$

$$\left(h_{out} + \frac{w_{out}^2}{2} \right) = e \neq const. \quad \text{not constant total spec. enthalpy} \quad (5.3)$$

$$\frac{dm_{cha}}{m_{cha}} = \frac{du_{cha}}{h_{out} + \frac{w_{out}^2}{2} - u_{cha}} \quad \text{chamber outflow equation} \quad (5.4)$$

• Liquid outflow

$$T_{cha,L,2} = T_{cha,L,1} + \frac{w_{out}^2}{2 \cdot c_{v,L}} \cdot \ln \left(\frac{m_{cha,L,2}}{m_{cha,L,1}} \right) \quad (5.5)$$

• Gas expansion by liquid outflow

$$V_{cha,G,1} = \alpha_{cha,2} \cdot V_{cha} - \frac{\Delta m_{out,L}}{\rho_L} \quad \text{gas volume - before} \quad (5.6)$$

$$V_{cha,G,2} = \alpha_{cha,2} \cdot V_{cha} \quad \text{gas volume - after} \quad (5.7)$$

$$p_2 = p_1 \cdot \left(\frac{V_{cha,G,1}}{V_{cha,G,2}} \right)^\kappa \quad \text{isentropic change of pressure} \quad (5.8)$$

$$T_{G,2} = T_{G,1} \cdot \left(\frac{V_{cha,G,1}}{V_{cha,G,2}} \right)^{(\kappa-1)} \quad \text{isentropic change of temp.} \quad (5.9)$$

• **Gas outflow**

$$\frac{m_{cha,G,2}}{m_{cha,G,1}} = \left(\frac{\frac{W_{out}^2}{2} + R \cdot T_{cha,G,2}}{\frac{W_{out}^2}{2} + R \cdot T_{cha,G,1}} \right)^{\left(\frac{1}{\kappa-1} \right)} \quad \text{resulting in} \quad T_{cha,G,2} \quad (5.10)$$

$$\frac{m_{cha,G,2}}{m_{cha,G,1}} = \frac{p_{cha,2} \cdot T_{cha,G,1}}{p_{cha,1} \cdot T_{cha,G,2}} \quad \text{resulting in} \quad p_{cha,2} \quad (5.11)$$

6. Gas-liquid heat transfer inside a single chamber

After the chamber inflow and outflow process, a time-dependent mutual heat transfer [6] through the interfacial area between remaining fractions of the liquid and gaseous phase lead to a partial temperature or energy balancing. Generally, the temperature of the gaseous phase will decrease and the liquid phase will be heated up. After defining a time span - the heat transfer duration is equal to a single time step - and the initial conditions for the temperatures of the liquid and the gaseous phase, a system of ordinary differential equations has to be solved. The heat fluxes for both phases as well as the heat transfer flux through the interfacial area can be defined as

$$\dot{Q}_L = m_L \cdot c_L \cdot \frac{dT_L}{dt} \quad \text{Heat flux of the liquid phase} \quad (6.1)$$

$$\dot{Q}_G = m_G \cdot c_{p,G} \cdot \frac{dT_G}{dt} \quad \text{Heat flux of the gaseous phase} \quad (6.2)$$

$$\dot{Q}_{HT} = h_{HT} \cdot A_{HT} \cdot (T_G - T_L) \quad \text{Heat transfer flux through the interfacial area} \quad (6.3)$$

The system of ordinary differential equations, which results from the equating of Equations (6.1) and (6.2) with Equation (6.3), has the following form:

$$\frac{dT_L}{dt} = \frac{h_{HT} \cdot A_{HT}}{m_L \cdot c_L} \cdot (T_G - T_L) \quad (6.4)$$

$$\frac{dT_G}{dt} = \frac{h_{HT} \cdot A_{HT}}{m_G \cdot c_{p,G}} \cdot (T_L - T_G) \quad (6.5)$$

The greatest problems in determining the mutual heat transfer and thus the temperature of both phases as a function of time is the correct definition of the heat transfer coefficient and the interfacial area. The latter depends mainly on the kind of the current multiphase flow pattern inside the chamber, which can develop

from a simple stratified flow to highly dispersed liquid drops in the gaseous phase. Therefore, a correlation must still be found, which takes the different flow patterns and the corresponding heat transfer coefficients into consideration. Because of the present lack of knowledge concerning the mutual phase heat transfer coefficients and the interfacial area, the product of both parameters was chosen in a way, that the total heat balance was reached during a single time step, so that both phase temperatures will be identical at the end of the heat transfer. The Figure 6.1 shows the time-dependent phase temperatures during the mutual heat transfer process inside the last chamber near by the discharge port.

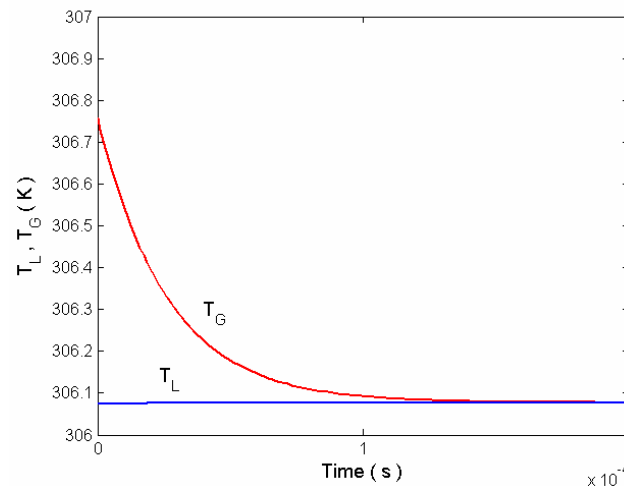


Figure 6.1 : Time-dependent heat transfer between the liquid and gaseous phase

7. The multiphase pressure-driven gap flows

• The perimeter and radial gap

The perimeter gap, shown in the left hand side of Figure 7.1 and in Figure 1.1, is the distance between the outer screw diameter and the inner diameter of the housing and it connects two chambers back-to-back. Because of the large outer screw diameter compared with the absolute gap height, the curvature of the gap can be neglected, so that it can be treated as a rectangular clearance. The radial gap, shown in the right hand side of Figure 7.1 as well as in Figure 1.1, is the space between the outer and the inner radius of the screws. Dependent upon the number of flights, it connects two chambers back-to-back or one chamber with the next but one. The basic theory of the perimeter gap is also valid for the radial gap. Only the geometric boundary conditions are different.

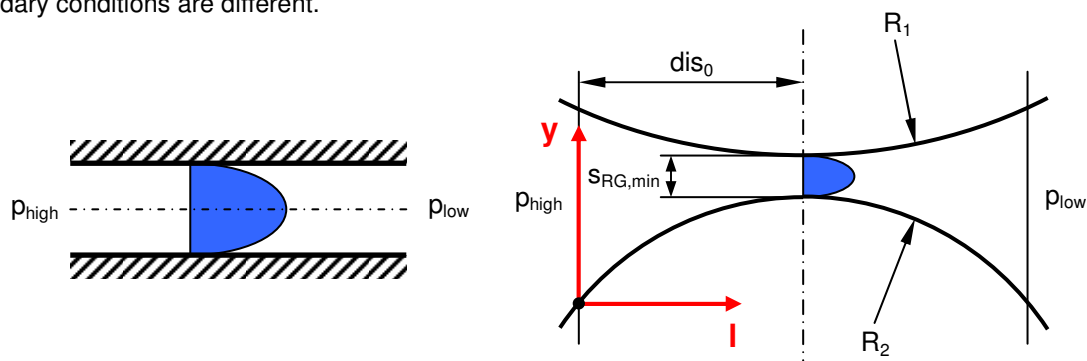


Figure 7.1 : The compressible pressure-driven flow inside the perimeter gap (left) and the radial gap (right)

To change the former incompressible single-phase equations into a compressible gap flow formulation, the Homogeneous Equilibrium Model [9], [10] and [11] for multiphase flows, where both phases have the same pressure, velocity, and temperature at an arbitrary position of the gap, was used. The steady state conservation equations - adiabatic flow with a negligible change of potential energy - for a constant or also variable gap height along the flow path follow to:

$$\frac{\partial(\rho_H \cdot w \cdot s)}{\partial l} = 0 \quad \text{Conservation of mass} \quad (7.1)$$

$$\frac{\partial p}{\partial l} + \frac{1}{s} \cdot \frac{\partial(\rho_H \cdot w^2 \cdot s)}{\partial l} + \lambda \cdot \frac{\rho_H}{4 \cdot s} \cdot w^2 = 0 \quad \text{Conservation of momentum} \quad (7.2)$$

$$\frac{dT}{dl} + \frac{1}{c_{p,H}} \cdot w \cdot \frac{dw}{dl} = 0 \quad \text{Conservation of energy} \quad (7.3)$$

The friction factor in Equation (7.2) was defined for laminar and rough turbulent flows, depending on the according Reynolds number inside the perimeter or radial gap. To define the mass fraction or the homogeneous density of the fluid at the gap inlet, a new correlation was developed, which relates the gas volume fraction at the suction side (global GVF) of the screw pump to the GVF at the corresponding gap inlet. The correlation presents a smooth transition from a liquid single phase leakage flow, which still exists at a global GVF of approx. 85 %, to a purely gaseous backflow at a global GVF of 100 %.

• Solution of the conservation equations as a system of ordinary differential equations

For a convenient solution of the ODE system, the conservation equations were transformed into a matrix formulation, see also Equations (7.4) to (7.7), and afterwards solved by a fourth-order Runge-Kutta scheme. All primitive variables are solved simultaneously from the gap inlet step-wise to the gap outlet.

$$\mathbf{A} \cdot \frac{\partial \mathbf{X}}{\partial l} = \mathbf{b} \quad (7.4)$$

$$\mathbf{A} = \begin{bmatrix} \frac{x \cdot R \cdot T \cdot w \cdot \rho_H^2}{p^2} & \rho_H & -\frac{x \cdot R \cdot w \cdot \rho_H^2}{p} \\ 1 & \rho_H \cdot w & 0 \\ 0 & w & c_{p,H} \end{bmatrix} \quad (7.5)$$

$$\mathbf{X} = \begin{bmatrix} p \\ w \\ T \end{bmatrix} \quad (7.6) \quad \mathbf{b} = \begin{bmatrix} -\frac{ds}{dl} \cdot \rho_H \cdot w / s \\ -\lambda \cdot \rho_H \cdot w^2 / (4 \cdot s) \\ 0 \end{bmatrix} \quad (7.7)$$

The following Figures 7.2 and 7.3 present exemplary distributions of the three primitive variables pressure, mean velocity and temperature as well as the distributions of the coefficient matrix determinant firstly for the perimeter gap and secondly for the radial gap.

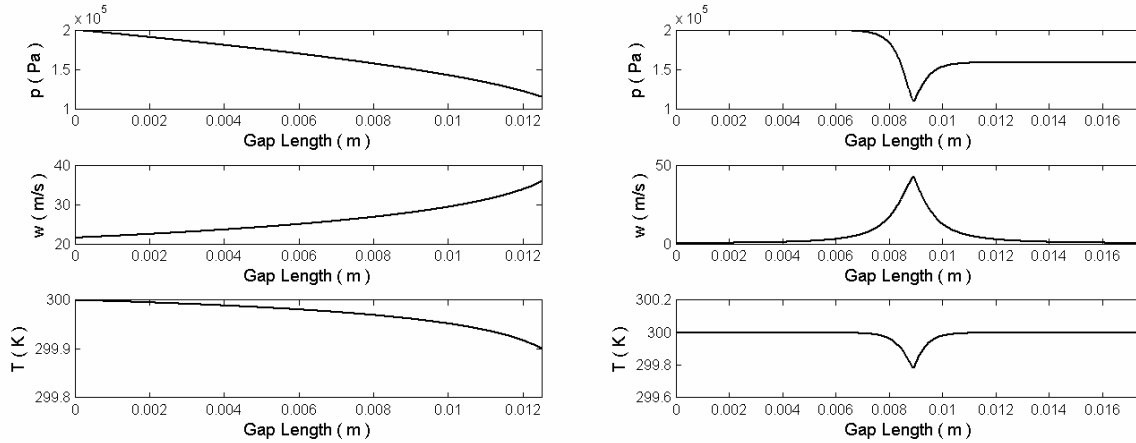


Figure 7.2 : Distributions of the primitive variables inside the perimeter gap (left) and the radial gap (right)

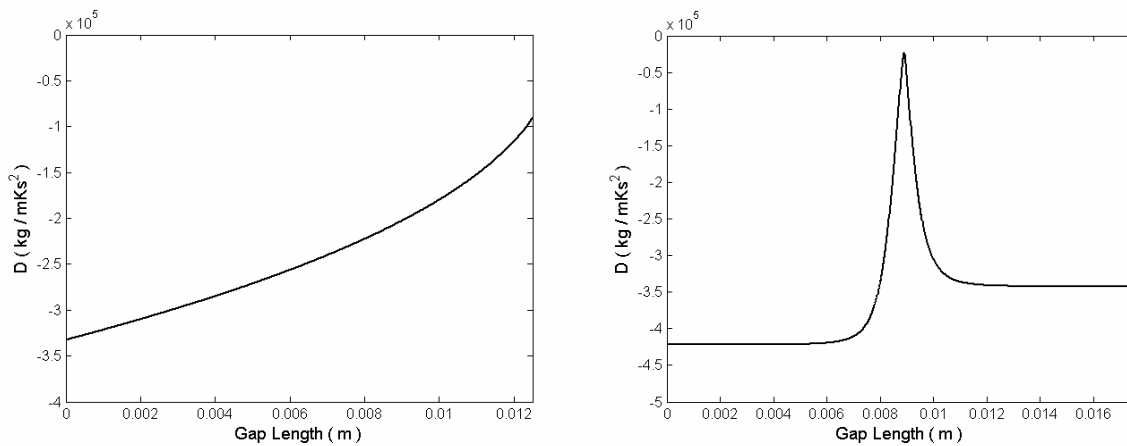


Figure 7.3 : Distributions of the coefficient matrix determinants inside the perimeter gap (left) and the radial gap (right)

The advantage of this matrix formulation is the fact that the coefficient or the left-hand side matrix \mathbf{A} of the system of conservation equations serves as an indicator for the critical flow condition. If the gap flow reaches anywhere the critical speed, the pressure gradient will be infinite at this location. Simultaneously, the determinant of matrix \mathbf{A} will become zero. Therefore, the inlet velocity must be increased step by step until the determinant of the coefficient matrix will be zero, then the critical mass flux density is determined. The perimeter gap and the radial gap are both affected by this critical flow effects. For the screw pump model it will be assumed, that the critical speed or the critical pressure is reached at the perimeter gap outlet or the radial gap nip region.

8. Optimisation or adjustment of the gap inflow velocity

In the case of the compressible perimeter and radial gap flow, the application of boundary conditions at the gap inlet and outlet is not possible. In the one-dimensional incompressible case, the mean velocity can be determined by the gap pressure difference and the friction factor. In the compressible case however, only boundary conditions at the inlet could be applied. In contrast to the thermodynamic variables inlet pressure and temperature, the inlet velocity is unknown. But there is an additional variable, which is known: the outlet pressure or the pressure of the next chamber. Therefore, it is possible to estimate an inlet velocity and calculate the corresponding outlet pressure and iterate the process until the calculated outlet pressure is equal to the pressure of the next chamber. To make this iteration process faster and more efficiently, an optimisation process, see Figure 8.1, is used.

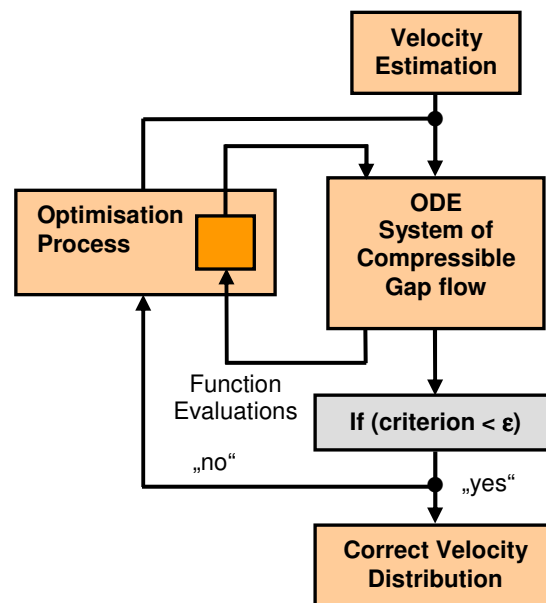


Figure 8.1 : Scheme of inflow velocity adjustment

The optimisation algorithms, which are used to optimise a system or to minimise a criterion, depend on the kind of system equations (linear or non-linear) and on restrictions for the optimisation variables. Very popular and also efficient algorithms are the Quasi-Newton method (Fletcher, Powell) for non-restrictive optimisation problems and the Sequential Quadratic Programming (Powell, Schittkowski) for more complex and restrictive problems, which are both available in the mathematical programme system MATLAB. An advantage of the Quasi-Newton method is the insensitivity towards initial conditions for the optimisation variables, which are located far away from the minimum. This is the reason, that this method is often preferred for global optimisation problems.

The optimisation variable is the inflow velocity w_0 , for which additional informations like initial conditions, upper and lower bounds have to be defined. The optimisation criterion, which has to be minimised, is the difference between the calculated outlet pressure and the actual pressure in the next chamber:

$$f_{crit} = |p_{outlet} - p_{cha,real}| \quad (8.1)$$

But for critical compressible flows, it must be considered, that the pressure difference criterion is not valid anymore, if the critical mass flux is reached. A further pressure reduction will not cause an increase of the inlet velocity, so that the velocity has to be fixed, if the determinant of the coefficient matrix decreases to zero at the perimeter gap outlet or the radial gap nip region.

9. Results of the screw pump simulation

The following exemplary multiphase screw pump simulation investigates an arbitrary operating point with an overall differential pressure of 10 bar, a global gas volume fraction of 96 % and a rotational speed of 2900 rpm. This rotational period is characterised by three closed chambers between the discharge and the suction side, in contrast to two closed chambers during the rest of a single rotation. The inflow temperature at the suction side was set to 300 K for both phases. The most important geometric parameters of the screw pump can be taken from Table 9.1.

Description	Symbol	Value	Unit
Outer screw diameter	D	100	mm
Inner screw diameter	d	70	mm
Thread pitch	h	50	mm
Screw length	l_s	120	mm
Number of flights	N	2	---
Chamber volume	V_{cha}	44	cm ³
Perimeter gap height	s_{PG}	188	μm
Min. radial gap height	s_{RG}	105	μm

Table 9.1: Important geometric parameters

The pressure distribution inside the screw pump is presented by Figure 9.1. The horizontal steps indicate the homogeneous pressure field inside each chamber. Above a GVF of approx. 85 %, the pressure distribution is losing step by step the former parabolic shape, which had a large pressure gradient near by discharge side. At a GVF of 96 %, the leakage flow is already characterised by two phases and has a decreasing density and viscosity, so that the sealing behaviour is also decreasing. As the backflow increase, the pressure rises in each chamber and the pressure profile returns to linearity.

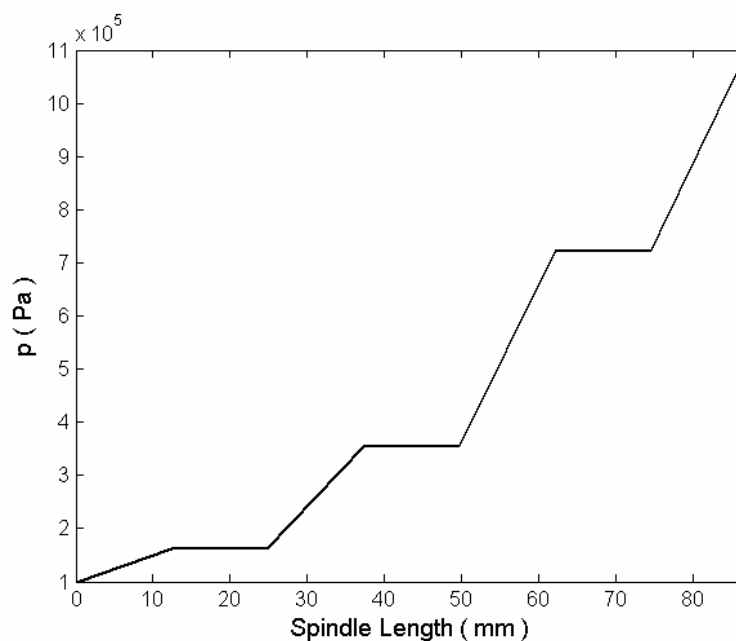


Figure 9.1 : Pressure distribution inside the screw pump

Figure 9.2 and 9.3 are showing the thermodynamic behaviour of the liquid and the gaseous phase between the suction and the discharge port. The largest gradient at this high GVF is occurring between the suction side and the first chamber, because of the backflow of already heated fluid from the discharge into the different chambers. At the moment, where the last chamber opens to the discharge port, the remaining gas phase is compressed by the fast expanding fluid of the discharge, so that the gas temperature will be increased again, before the chamber content is released to the high pressure side.

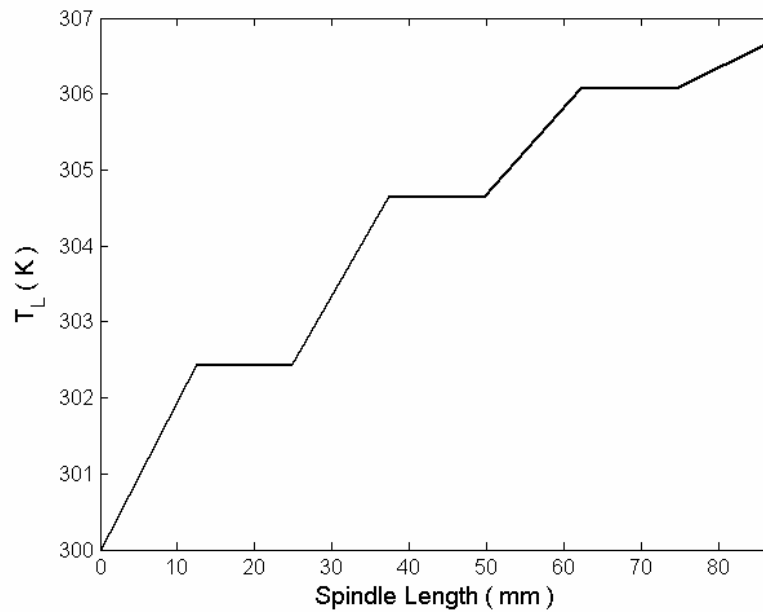


Figure 9.2 : Liquid temperature distribution inside the screw pump

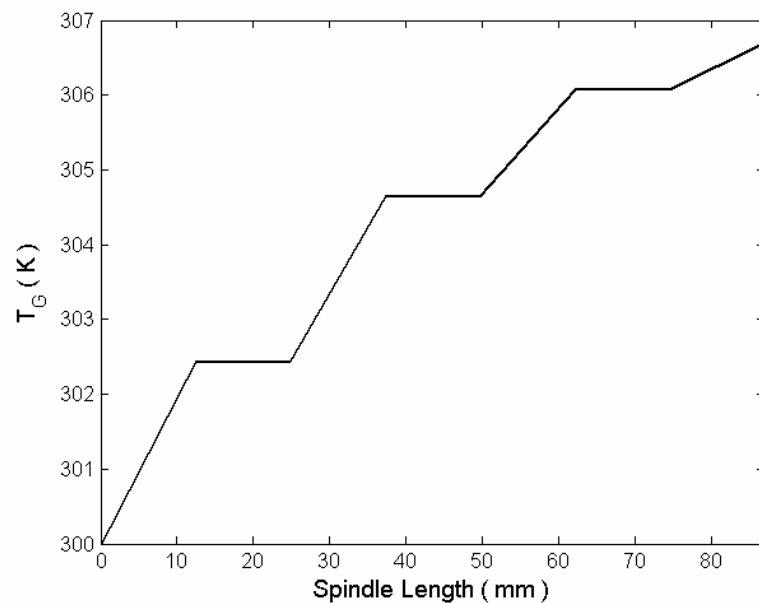


Figure 9.3 : Gas temperature distribution inside the screw pump

The gas densities as well as the gas volume fractions in each chamber are presented by the two following Figures 9.4 and 9.5. The gas densities are simply determined by the chamber pressure, the gas temperature and the use of the equation of state for air as an ideal gas. While the gas densities are increasing along the conveyance direction, the GVF's are decreasing because of the backflow of the liquid phase and the resulting compression of the gaseous phase.

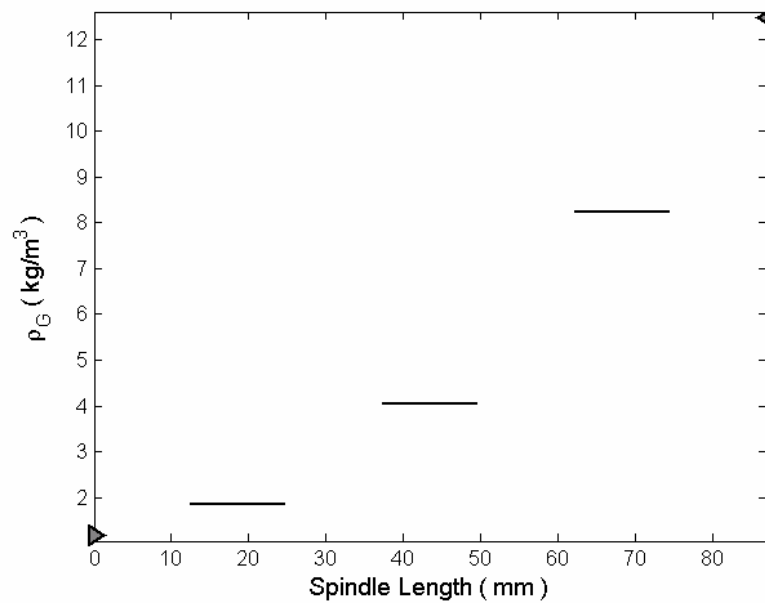


Figure 9.4 : Chamber gas densities inside the screw pump

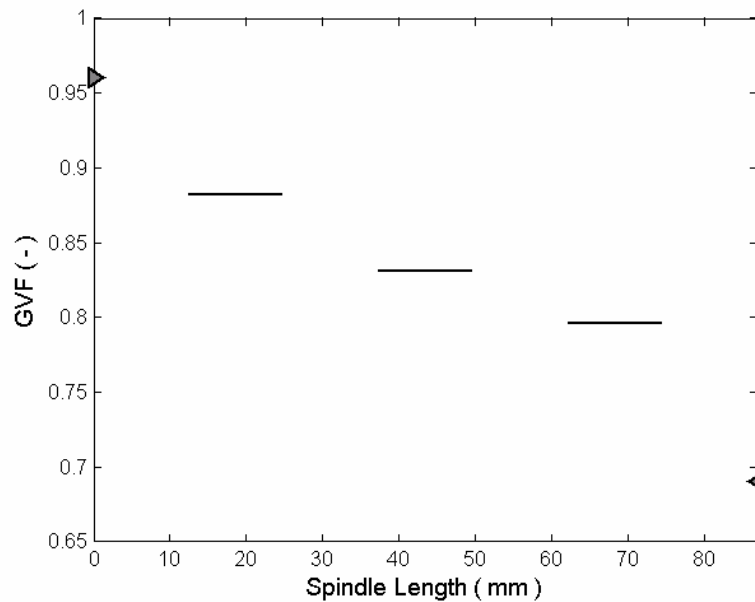


Figure 9.5 : Chamber GVF's inside the screw pump

Figure 9.6 shows the convergence of the volumetric efficiency as a function of chamber changes. After approx. 60 chamber iteration loops or 30 spindle rotations, a steady state is reached. Figure 9.7 presents the residual histories of the chamber pressure and both phase temperatures for the last chamber near by the discharge port as an example. The residuals are the differences of a certain variable between two consecutive chamber changes and have to decrease in time in order to obtain good convergence behaviour. The chamber pressure converges after only 7 iterations, whereas both temperatures converge after 45 chamber changes.

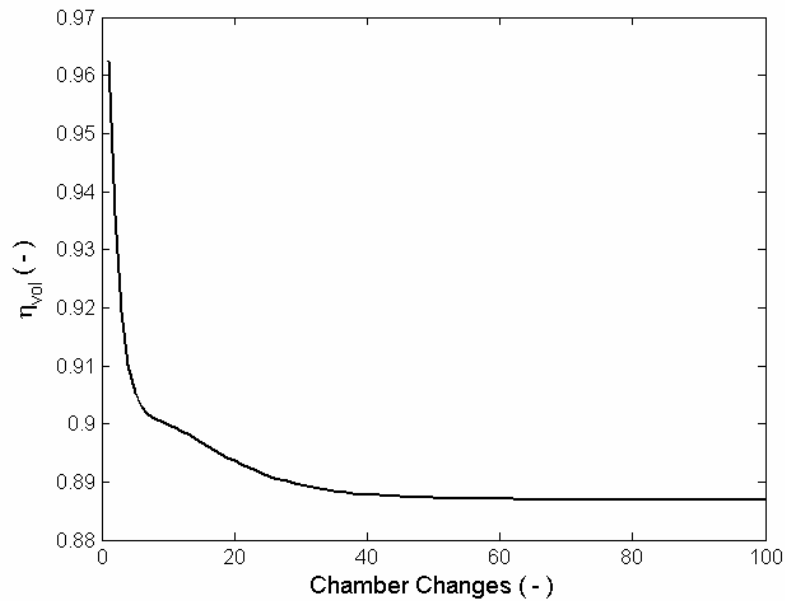


Figure 9.6 : Convergence history of the volumetric efficiency

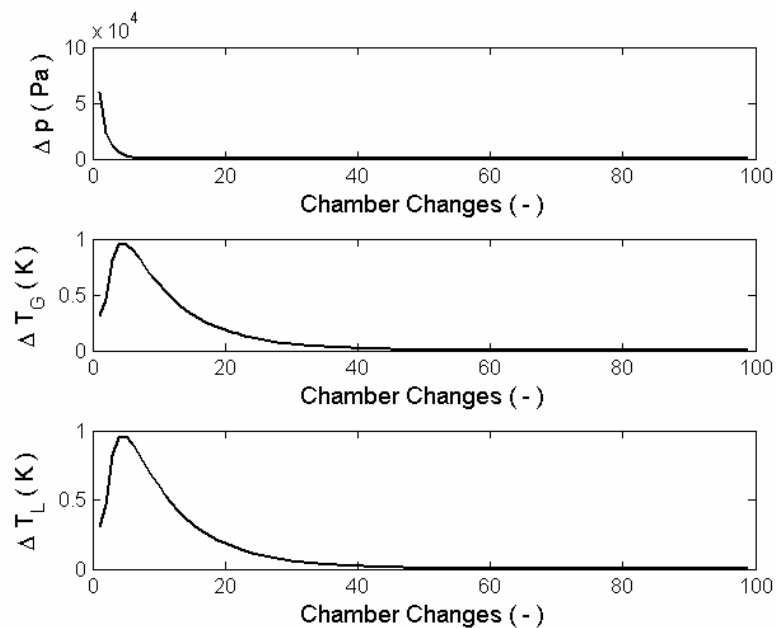


Figure 9.7 : Residual histories of the pressure and phase temperatures of the last chamber

The volumetric efficiency during a conveyance period of three closed chamber is equal to 88.7 %, which can be also seen by the steady state in Figure 9.6. Weighting both numbers of existing chambers to calculate the real leakage volume flow, will result in an integral real volume flow of 39.4 m³/h. Considering the theoretical volume flow of 61.2 m³/h, this would correspond to a final volumetric efficiency of 64.4 %.

10. Conclusion

The presented multiphase screw pump model was developed for the prediction of the pump conveyance behaviour especially at very high gas volume fractions above 85 %. To satisfy also the physical requirements on a multiphase, an almost purely gaseous flow, and compressible leakage flow, a new multiphase gap flow sub-model was introduced. This model is able to take into account the compressibility and acceleration effects of the leakage flow. The model is also capable of dealing with an extreme condition of critical flow, which can occur in a gap between two chambers having a large difference of static pressure. The consideration of these effects allows a more precise simulation of the thermodynamic behaviour and pump characteristics at very high gas volume fractions up to the conveyance break-off.

Acknowledgements

The authors would like to thank the company LEISTRITZ for all the information about multiphase screw pumps and their additional technical support and also the Department of Mechanical and Utility Engineering of the University of Applied Sciences in Nuremberg for the computational assistance and facilities.

Nomenclature

General symbols

A	area (general)
c	specific heat capacity
d	inner screw diameter
D	outer screw diameter , determinant
e	specific total enthalpy
E	energy (general)
f	criterion function
g	gravitational acceleration
h	specific enthalpy , heat transfer coefficient , thread pitch
H	enthalpy , height
l	length
m	mass
N	number of flights
p	static pressure
q	specific heat energy
Q	heat energy
R	individual gas constant , radius
s	gap height , specific entropy
t	time
T	temperature
u	specific internal energy
U	internal energy
v	specific volume
V	volume (general)
w	gap flow velocity
W	work energy
x	mass fraction
x,y,z	coordinate directions

Vectors / Matrices

A	coefficient matrix
b	right hand side vector
X	vector of primitive variables

Greek Letters

α	gas volume fraction
Δ	difference
ε	small criterion value
η	efficiency
κ	isentropic exponent
λ	friction factor
ρ	density

Subscripts

cha	chamber
crit	criterion
G	gaseous
h	hydraulic
H	homogeneous
HT	heat transfer
in	inflow
kin	kinetic
L	liquid
min	minimum
out	outflow
p	constant pressure
pot	potential
S	screw
tech	technical
v	constant volume
vol	volumetric
0	initial condition

Abbreviations

dis	distance
D	discharge
GVF	gas volume fraction
ODE	ordinary differential equation
PG	perimeter gap
RG	radial gap
S	suction

References

- [1] WINCEK, M.:
Zur Berechnung des Förderverhaltens von Schraubenspindelpumpen bei der Förderung von Flüssigkeits / Gas-Gemischen, Dissertation, Universität Erlangen-Nürnberg, 1992
(*The calculation of the conveyance behaviour of screw pumps at the conveyance of liquid/gas-mixtures, Ph.D. thesis, University of Erlangen-Nuremberg, 1992*)
- [2] KÖRNER, H.:
Zum Förderverhalten von Schraubenspindelpumpen für Zweiphasengemische hohen Gasgehalts, Dissertation, Universität Erlangen-Nürnberg, 1998
(*The conveyance behaviour of screw pumps for two-phase mixtures with high gas-volume-fractions, Ph.D. thesis, University of Erlangen-Nuremberg, 1998*)
- [3] ETZOLD, S.:
Verlustanalyse von Schraubenspindelpumpen bei Mehrphasenförderung, Dissertation, Universität Hannover, 1993
(*Leakage analysis of screw pumps during multiphase conveyance, Ph.D. thesis, University of Hanover, 1993*)
- [4] NAKASHIMA, C.Y. / OLIVEIRA, S. / CAETANO, E.F.:
Thermo-hydraulic model of a twin-screw multiphase pump, ASME IMECE 04, Anaheim, USA, 2004
- [5] RAUSCH, T. / VAUTH, T. / BRANDT, J.U. / MEWES, D.:
A model for the delivering characteristic of multiphase pumps, 4th North American Conference on Multiphase Technology, Banff, Canada, 2004
- [6] STEPHAN, K. / MAYINGER, F.:
Thermodynamik - Grundlagen und technische Anwendungen - Band 1 Einstoffsysteme, Springer-Verlag, Berlin / Heidelberg, 1986
(*Thermodynamics - fundamentals and technical applications - vol. 1 single material systems*)
- [7] HAHNE, E.:
Technische Thermodynamik - Einführung und Anwendung, Addison-Wesley, Bonn, 1993
(*Technical thermodynamics - introduction and application*)
- [8] WAGNER, W.:
Wärmeübertragung, Vogel Verlag, Würzburg, 1998
(*Heat transfer*)
- [9] WALLIS, G.B.:
One-dimensional Two-phase Flow, McGraw Hill Inc., 1969
- [10] LEVY, S.:
Two-phase flow in complex systems, John Wiley & Sons, New York, 1999
- [11] MAYINGER, F.:
Strömung und Wärmeübergang in Gas-Flüssigkeits-Gemischen, Springer-Verlag, Wien / New York, 1982
(*Flow and heat transfer in gas-liquid mixtures*)
- [12] BESTLE, D.:
Analyse und Optimierung von Mehrkörpersystemen, Springer-Verlag, Berlin / Heidelberg, 1994
(*Analysis and optimization of multi-body systems*)
- [13] CORRADINI, M.L.:
Multiphase Flow : Gas/Liquid (*The Handbook of Fluid Dynamics*), ed. R. W. Johnson, CRC Press LLC / Springer-Verlag, Boca Raton / Heidelberg, 1998